

Sparsity-Based Frequency-Hopping Spectrum Estimation with Missing Samples

Shengheng Liu^{†‡}, Yimin D. Zhang[‡], and Tao Shan[†]

[†]School of Information and Electronics, Beijing Institute of Technology, Beijing 100081, China

[‡]Department of Electrical and Computer Engineering, Temple University, Philadelphia, PA 19122, USA

Abstract—In this paper, we address the problem of spectrum estimation of frequency-hopping (FH) signals in the presence of random missing samples. The signals are analyzed within the bilinear time-frequency representation framework, where a time-frequency kernel is designed based on inherent FH signal structures. The designed kernel permits effective suppression of cross-terms and artifacts due to missing samples while preserving the FH signal auto-terms. The kernelled results are represented in the instantaneous autocorrelation function domain, which are then processed using sparse reconstruction methods for high-resolution estimation of the FH signal time-frequency spectrum. The proposed method achieves accurate FH signal spectrum estimation even when a large proportion of data samples is missing. Simulation results verify the effectiveness of the proposed method and its superiority over existing techniques.

Keywords—Frequency hopping, spectrum estimation, missing samples, sparse reconstruction, time-frequency distribution, kernel design

I. INTRODUCTION

Frequency-hopping (FH) signals are generated by varying the carrier frequencies according to a certain hopping pattern. Due to their inherent capability of low probability of intercept and resistance to jamming and multipath fading, FH signals have been widely utilized in radar, communication, and satellite navigation. FH signals are a popular choice of waveforms for single-platform and multiple-input multiple-output (MIMO) radar systems [1]–[4]. In order to improve MIMO radar system resolution, a set of FH pulses are designed in [5] based on simulated annealing algorithm to optimize the MIMO radar ambiguity function (AF). A modular software-defined FH radar is developed in [6] for through-wall imaging and motion detection at a significant standoff distance. Multiple-target motion parameters are estimated based on sparse modeling via a colocated MIMO FH radar [7].

For a variety of applications ranging from interception of non-cooperative emitters to exploitation of signals of opportunity for passive sensing, and to design strategies for spectrum sharing between different wireless communication and sensing platforms, estimating and tracking the hopping spectrum of FH signals are of significant interest. However, this task is often challenging when the hopping patterns of the constituent signals are unknown, particularly from highly noisy observations [8].

As FH signals generally exhibit sparsity in the joint time-frequency domain, compressive sensing (CS) and sparse reconstruction techniques [9], [10] can be used to robustly recover their spectrum with fewer and even corrupted samples. In the

CS context, FH parameters can be estimated by formulating the problem as an underdetermined linear regression with a dual sparsity penalty [8], [11]. To improve performance, particularly in low signal-to-noise ratio (SNR) conditions, a sparse Bayesian learning-based approach was proposed in [12]. Nevertheless, these approaches are based on linear time-frequency analysis and suffer from temporal-spectral resolution trade-offs, resolution restraint due to the uncertainty principle, and none considered the effect of missing samples.

In practice, the received signals are often subject to missing samples, which may arise from fading, obstruction, impulsive noise, and collecting/storage equipment failures, leading to degraded FH spectrum estimation performance. Recent results have shown that missing samples generate strong undesirable artifacts in the time-frequency domain, thus making the conventional time-frequency analysis and sparse reconstruction methods difficult to apply [13]. The effect of missing samples on the time-frequency distribution and robust recovery using time-frequency kernels and sparse reconstruction were first reported in [14].

In this paper, we develop a new approach for FH spectrum estimation based on bilinear time-frequency representations (TFRs) under the sparse reconstruction framework. In the context of bilinear TFRs, the ambiguity domain representation of the FH signals allows convenient FH signal auto-term selection that enables effective suppression of undesirable artifacts as well as cross-terms. The results are then used for sparse reconstruction of the TFRs by utilizing the linear Fourier relationship between the kernelled instantaneous autocorrelation function (IAF) and the TFRs. As such, the proposed approach can robustly restore the FH spectrum in noisy and missing sample case without the requirement of *a priori* information of the hopping patterns. The advantage of the FH signal structure-aware kernel outperforms the adaptive optimal kernel (AOK), particularly under severe conditions with a high level of noise and/or a high number of missing samples.

Notations: Lower-case (upper-case) bold characters are used to denote vectors (matrices). $\text{abs}(\cdot)$ returns the modulus of a given complex number. \circ denotes Hadamard product. $\text{diag}\{\cdot\}$ represents a diagonal matrix that uses the entries of a vector as its diagonal entries, and \mathbf{I}_N denotes an $N \times N$ identity matrix. $(\cdot)^*$, \mathbf{F}_d and \mathbf{F}_d^{-1} denote the one dimensional discrete Fourier transform (DFT) and inverse discrete Fourier transform (IDFT) matrices with respect to the d dimension, respectively. $(\cdot)^T$ and $(\cdot)^H$ respectively denote complex conjugate, transpose and hermitian operations of a matrix. $\|\cdot\|_p$ represents the ℓ_p -norm of a vector, and $|\cdot|$ denotes the cardinality of a set.

II. SIGNAL MODEL

Consider a discrete-time FH signal $\tilde{\mathbf{s}}[n]$, corrupted by additive complex white Gaussian noise, expressed as [11], [12],

$$\tilde{\mathbf{s}}[n] := \sum_{k=1}^{K_l} A_{k,l} e^{j2\pi f_{k,l} n / f_s} + \mathbf{v}[n], \quad n_{l-1} \leq n < n_l, \quad (1)$$

where n_l is the l -th system-wise hopping instant, $A_{k,l}$ and $f_{k,l}$ are the complex amplitude and frequency of the k -th tone in the l -th system dwell $[n_{l-1}, n_l]$, respectively, where $l = 1, 2, \dots, L$, and L denotes the total number of system-wise hops. The observed data length is N , and the number of tones K_l can vary with l because of emitter (de)activation or bandwidth mismatch [8]. In addition, f_s is the sampling rate, and $\mathbf{v}[n]$ is the noise vector.

Denote $\mathbf{x}[n]$ as the observation data with $N - M$ missing samples, and the positions of these missing samples are assumed to be randomly distributed. As such, $\mathbf{x}[n]$ can be regarded as the Hadamard product of $\tilde{\mathbf{s}}[n]$ and an binary mask $\mathbf{b}[n]$, i.e.,

$$\mathbf{x}[n] = \tilde{\mathbf{s}}[n] \circ \mathbf{b}[n], \quad (2)$$

with

$$\mathbf{b}[n] := \begin{cases} 1, & \text{if } n \in \mathcal{J}, \\ 0, & \text{otherwise,} \end{cases} \quad (3)$$

where $\mathcal{J} \subset \{1, 2, \dots, N\}$ is the set of observed time instants with cardinality $|\mathcal{J}| = M$, and M/N represents the missing-sample ratio.

III. PROPOSED FH SPECTRUM ESTIMATION APPROACH

A. Bilinear Time-Frequency Representations

The discrete IAF of a signal $x[n]$, $n = 1, 2, \dots, N$, is defined as

$$C_{xx}[\tau, n] = x[n + \tau] x^*[n - \tau], \quad (4)$$

where τ denotes the time lag index.

Stack $C_{xx}[\tau, n]$ corresponding to all values of τ and n as a matrix \mathbf{C}_{xx} . Then, the AF matrix of signal $\mathbf{x} = [x(1), \dots, x(N)]^T$, expressed with respect to lag τ and Doppler frequency κ , can be obtained by performing IDFT of the IAF with respect to the time index n , i.e.,

$$\mathbf{A}_{xx}\{\tau, \kappa\} = \mathbf{F}_n^{-1} \mathbf{C}_{xx}\{\tau, n\} = \sum_n \mathbf{C}_{xx}\{\tau, n\} e^{j2\pi \kappa n}, \quad (5)$$

where the notation $\{\tau, \kappa\}$ is used to emphasize that the matrix \mathbf{A}_{xx} is constructed with respect to variables τ and κ .

The Wigner-Ville distribution (WVD) can be obtained by performing DFT to its IAF with respect to the lag index τ , i.e.,

$$\mathbf{W}_{xx}\{f, n\} = \mathbf{F}_\tau \mathbf{C}_{xx}\{\tau, n\} = \sum_\tau \mathbf{C}_{xx}\{\tau, n\} e^{-j4\pi f \tau}. \quad (6)$$

B. Kernel Design Based on FH Signal Structures

For FH signals, the frequency spectra represented by the auto-term time-frequency distributions depend on the hop frequency and vary over time. As such, it is difficult to design a single filter or mask in the time-frequency domain for both linear and bilinear TFRs. However, when represented in the ambiguity domain, auto-terms of FH signals, and other nonstationary in general, always pass through the origin with

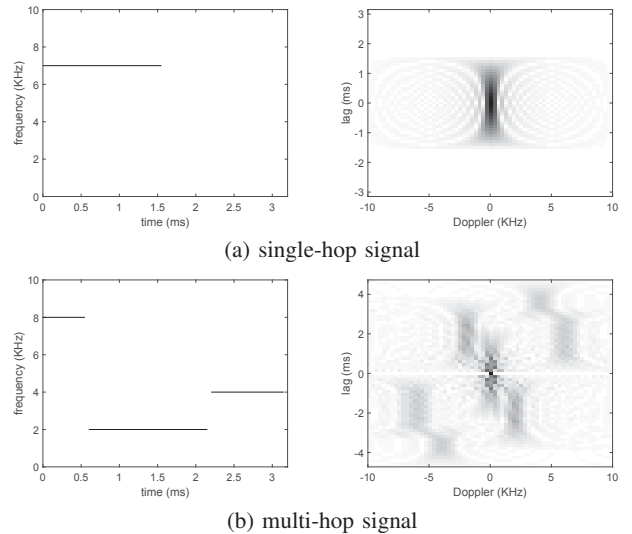


Fig. 1. Hopping frequency spectrum and AF of FH signals.

low-pass characteristics. On the other hand, cross-terms due to bilinear operation are positioned away from the ambiguity domain origin. This property has motivated a large amount of work to design time-frequency kernels for auto-term preservation and cross-term suppression [15], [16]. While a number of such kernels are available, data-dependent adaptive kernels, such as the adaptive optimal kernel (AOK) [17], are found attractive for this purpose because the kernels are adaptive tuned to optimize the preservation of signal auto-terms [14], [18]. Nevertheless, a critical problem with the AOK is that it may malfunction when the signals are highly contaminated by additive noise and artifacts due to missing samples.

We notice an important fact that, for the FH signals within each hop, their auto-terms are always present on the lag axis (i.e., zero zero-Doppler), regardless of their hop frequencies. Consider for example an single-hop FH signal with a sampling rate 20 KHz and hopping period of 1.6 ms, whose spectrum and AF are shown in Fig. 1(a). Note that the shape (magnitude) of the AF does not depend on the hopping frequency. On the other hand, for the multi-component shown in Fig. 1(b), the auto-terms remain in the same position (the exact value is distorted due to the superposition of multiple component) whereas the cross-terms appear away from the origin depending on the signal lags and the hop frequency difference. Note in Fig. 1(b) that we purposely used fractional hop period to emphasize that the hop period is not known. In addition, as we will see later, the effect of missing samples is manifested as artifacts spreading over the entire ambiguity domain. Based on this property, one can design a time-frequency kernel that utilize the known property of the FH signal auto-terms in the AF domain. The designed kernel will keep the auto-term ambiguity region while filtering out other ambiguity regions, reducing or eliminating, cross-terms and artifacts due missing samples.

In this paper, we design the kernel by thresholding the single-component auto-term AF, expressed as

$$\Psi[\tau, \kappa] = \begin{cases} |A_{xx}[\tau, \kappa]|, & \text{if } |A_{xx}[\tau, \kappa]| > \xi, \\ 0, & \text{otherwise,} \end{cases} \quad (7)$$

where ξ is the threshold, which is chosen to only keep FH auto-

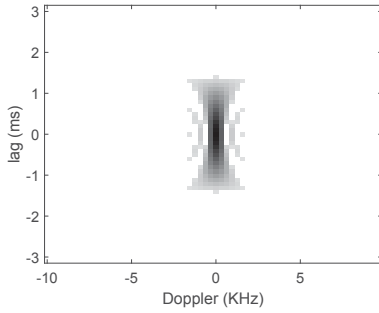


Fig. 2. Proposed ambiguity domain kernel.

term AF with substantial signal concentration. The resulting kernel function corresponding to the FH signal described above is shown in Fig. 2, where the value of ξ is chosen to be $0.125 \max[\mathbf{A}_{\text{xx}}\{\tau, \kappa\}]$.

C. Sparse Reconstruction of Time-Frequency Representations

The design kernel obtained in Section III-B is applied to the original AF, and the results are converted to the IAF domain through the Fourier transform with respect to the Doppler frequency κ , which can be expressed as follows

$$\mathbf{C}_{\text{xx}}\{\tau, n\} = \mathbf{F}_{\kappa} \tilde{\mathbf{A}}_{\text{xx}}\{\tau, \kappa\} = \mathbf{F}_{\kappa} (\mathbf{A}_{\text{xx}}\{\tau, \kappa\} \circ \Psi\{\tau, \kappa\}). \quad (8)$$

Note that the TFR matrix is associated with the resulting IAF matrix by the following Fourier relationship:

$$\mathbf{C}_{\text{xx}}\{\tau, n\} = \tilde{\Phi} \tilde{\mathbf{W}}_{\text{xx}}\{f, n\}, \quad (9)$$

where $\tilde{\Phi}$ is a Fourier transform matrix that perform IDFT with respect to frequency index f .

Denote the n th column of the IAF matrix $\mathbf{C}_{\text{xx}}\{\tau, n\}$ as $\mathbf{c}_{\text{xx}}[n]$, and the n th column of the bilinear TFR matrix $\tilde{\mathbf{W}}_{\text{xx}}\{f, n\}$ as $\mathbf{w}_{\text{xx}}[n]$. Then, their relationship, as depicted below, confirms the CS model in [19]:

$$\mathbf{c}_{\text{xx}}[n] = \tilde{\Phi} \mathbf{w}_{\text{xx}}[n], \quad (10)$$

Therefore, the TFR can be obtained from sparse reconstruction, in lieu of conventional Fourier transform, by repeating the procedure for each time instant column. Various compressive sensing algorithms can be used for this purpose. In this case, we use a simple form of orthogonal matching pursuit (OMP), which simply estimate the most likely frequency and its coefficient for each time instant. Other CS methods can be used as well.

IV. SIMULATION RESULTS AND ANALYSIS

Simulation results are provided to demonstrate the effectiveness of the proposed approach. In the simulations, we use an FH signal consisting of three components as depicted in Fig. 1(b). At the 20 KHz sampling rate, each hop of 1.6 ms yields 32 samples.

We first consider the situation where the input SNR is 0 dB, and 50% of the samples are randomly missing. The real-part waveform is shown in Fig. 3(a). The AF, IAF, and the WVD without applying a kernel are respectively shown in Fig. 3(b)–(d). It is clear that, because of the strong noise and large proportion of missing samples, no signatures can be

identified from the AF and WVD. Fig. 3(e)–(g) shows the AF, IAF, and TFR after the proposed kernel, as depicted in Fig. 2, is applied. Further, Fig. 3(h) shows the sparse TFR obtained from OMP, which shows clear and consistent FH spectrum. The comparison between Fig. 3(g) and Fig. 3(h) evidently shows the superiority of the sparse TFR reconstruction over the conventional Fourier based TFR.

Next, we compare with the performance of the AOK. Because the application of AOK fails to function in the above challenging situation, we shown in Fig. 4 a easier case where a higher SNR of 5 dB is assumed and only 20% samples are missing. Similarly, the waveform is shown in Fig. 4(a), and the unkernelled AF, IAF, and WVD are depicted in Fig. 4(b)–(d). The kernelled AF in Fig. 4(e) shows that it catches an undesired component due to cross-term effect, shown as a diagonal strip. As a result, both the Fourier-based TFR in Fig. 4(g) and the sparse TFR in Fig. 4(h) show incorrect spectrum estimates. By comparing the reconstruction results of Fig. 3(h) and Fig. 4(h), the advantages of the proposed kernel over the AOK is clearly demonstrated.

V. CONCLUSION

In this paper, a novel frequency hopping (FH) spectrum estimation approach with the consideration of missing samples was proposed within the framework of sparse reconstruction. In particular, a time-frequency kernel was designed that was constructed based on the inherent FH signal structure. The kernelled joint-variable representation over time and lag was used to provide the time-frequency signal representation through sparse reconstruction. It was shown that this approach outperforms existing approaches devised for the same problem.

ACKNOWLEDGMENT

The work of S.-H. Liu and T. Shan is supported in part by the National Natural Science Foundation of China under Grants No. 61331021 and 61421001. S.-H. Liu acknowledges the financial support from the China Scholarship Council for his stay at Temple University.

REFERENCES

- [1] S. V. Maric and E. L. Titlebaum, "A class of frequency hop codes with nearly ideal characteristics for use in multiple-access spread-spectrum communications and radar and sonar systems," *IEEE Trans. Commun.*, vol. 40, no. 9, pp. 1442–1447, Sep. 1992.
- [2] Y. Zhang and M. G. Amin, "MIMO radar exploiting narrowband frequency-hopping waveforms," in *Proc. European Signal Process. Conf.*, Lausanne, Switzerland, Aug. 2008, p. 1–5.
- [3] S. Badrinath, A. Srinivas, and V. U. Reddy, "Low-complexity design of frequency-hopping codes for MIMO radar for arbitrary Doppler," *EURASIP J. Adv. Signal Process.*, vol. 2000, article ID 319065, 14 pp.
- [4] K. Han and A. Nehorai, "Joint frequency-hopping waveform design for MIMO radar estimation using game theory, in *Proc. IEEE Radar Conf.*, Ottawa, Canada, April 2013, pp. 1–4.
- [5] C. Y. Chen and P. P. Vaidyanathan, "MIMO radar ambiguity properties and optimization using frequency-hopping waveforms," *IEEE Trans. Signal Process.*, vol. 56, no. 12, pp. 5926–5936, Dec. 2008.
- [6] A. R. Hunt, "Use of a frequency-hopping radar for imaging and motion detection through walls," *IEEE Trans. Geosci. Remote Sens.*, vol. 47, no. 5, pp. 1402–1408, May 2009.
- [7] S. Gogineni and A. Nehorai, "Frequency-hopping code design for MIMO radar estimation using sparse modeling," *IEEE Trans. Signal Process.*, vol. 60, no. 6, pp. 3022–3035, June 2012.

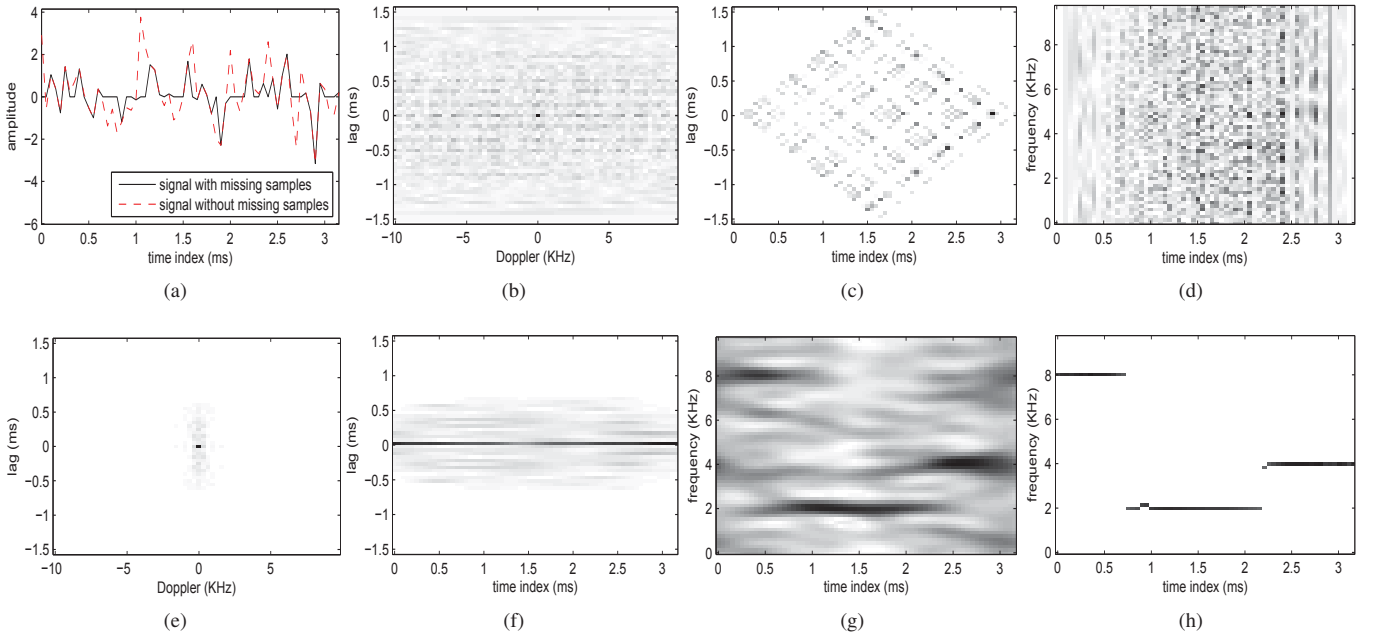


Fig. 3. Simulation results for the proposed kernel in a challenging scenario with 0 dB and 50% missing samples: (a) Time-domain waveform (real part) of the FH signal with or without missing samples; (b) unkernelled AF; (c) unkernelled IAF; (d) WVD; (e) kernelled AF; (f) kernelled IAF; (g) kernelled TFR obtained from Fourier transform; and (h) kernelled TFR obtained from OMP.

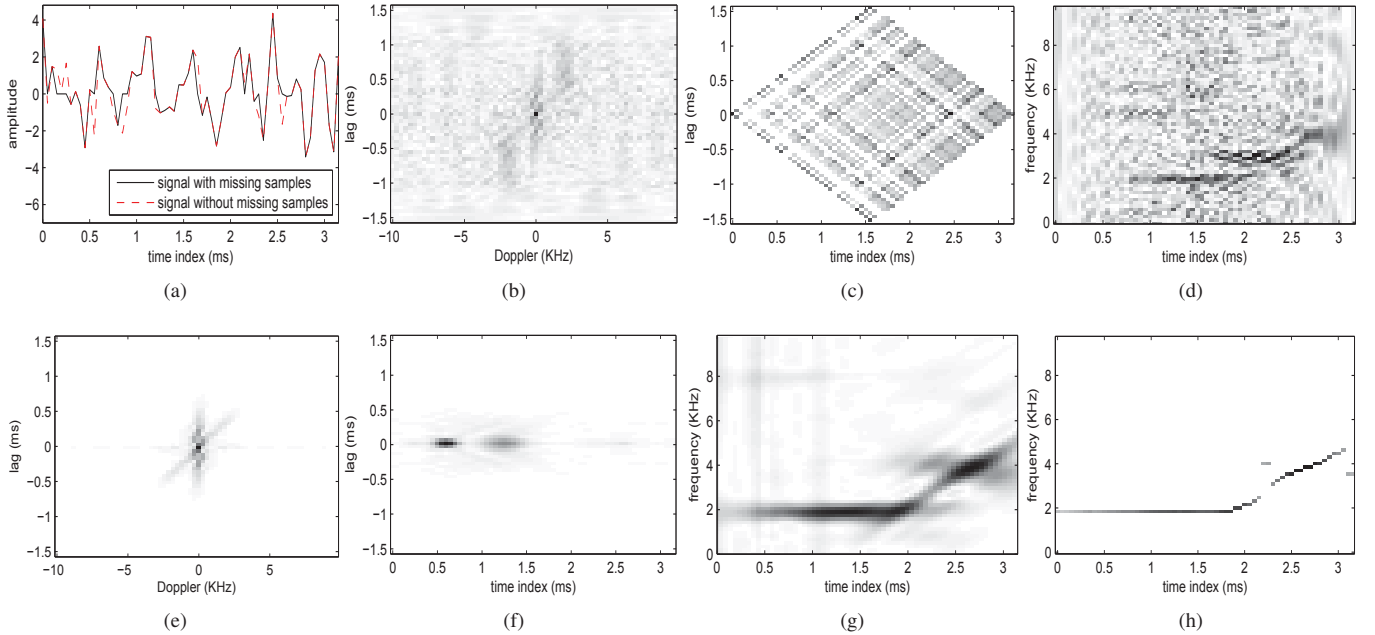


Fig. 4. Simulation results for the AOK in a less challenging scenario with 5 dB and 20% missing samples: (a) Time-domain waveform (real part) of the FH signal with or without missing samples; (b) unkernelled AF; (c) unkernelled IAF; (d) WVD; (e) kernelled AF; (f) kernelled IAF; (g) kernelled TFR obtained from Fourier transform; and (h) kernelled TFR obtained from OMP.

- [8] D. Angelosante, G. B. Giannakis, and N. D. Sidiropoulos, "Estimating multiple frequency-hopping signal parameters via sparse linear regression," *IEEE Trans. Signal Process.*, vol. 58, no. 10, pp. 5044–5056, Oct. 2010.
- [9] D. Donoho, "Compressed sensing," *IEEE Trans. Inform. Theory*, vol. 52, no. 4, pp. 1289–1306, Apr. 2006.
- [10] E. Candès, J. Romberg, and T. Tao, "Stable signal recovery from incomplete and inaccurate measurements," *Commun. Pur. Appl. Math.*, vol. 59, no. 8, pp. 1207–1223, Aug. 2006.
- [11] D. Angelosante, G. Giannakis, and N. Sidiropoulos, "Sparse parametric models for robust nonstationary signal analysis: Leveraging the power of sparse regression," *IEEE Signal Process. Mag.*, vol. 30, no. 6, pp. 64–73, Nov. 2013.
- [12] L.-F. Zhao, L. Wang, G.-A. Bi, L.-R. Zhang, and H.-J. Zhang, "Robust frequency-hopping spectrum estimation based on sparse Bayesian

- method," *IEEE Trans. Wireless Commun.*, vol. 14, no. 2, pp. 781–793, Feb. 2015.
- [13] L. Stankovic, S. Stankovic, I. Orovic, and Y. D. Zhang, "Time-frequency analysis of micro-Doppler signals based on compressive sensing," in M. Amin (ed.), *Compressive Sensing for Urban Radars*, CRC Press, 2014.
- [14] Y. D. Zhang, M. G. Amin, and B. Himed, "Reduced interference time-frequency representations and sparse reconstruction of undersampled data," in *Proc. European Signal Process. Conf.*, Marrakech, Morocco, pp. 1–5, Sep. 2013.
- [15] L. Cohen, *Time Frequency Analysis: Theory and Applications*, Prentice-Hall, 1994.
- [16] B. Boashash, *Time Frequency Signal Analysis and Processing: A Comprehensive Reference*, Elsevier, 2003.
- [17] D. L. Jones and R. G. Baraniuk, "An adaptive optimal-kernel time-frequency representation," *IEEE Trans. Signal Process.*, vol. 43, no. 10, pp. 2361–2371, Oct. 1995.
- [18] Q. Wu, Y. D. Zhang, and M. G. Amin, "Continuous structure based Bayesian compressive sensing for sparse reconstruction of time-frequency distributions," in *Proc. Int. Conf. Digital Signal Process.*, Hong Kong, China, Aug. 2014, pp. 831–836.
- [19] Y. C. Jones and G. Kutyniok, *Compressed Sensing*, Cambridge University Press, 2012.